11th World Congress on Structural and Multidisciplinary Optimisation
07th -12th, June 2015, Sydney Australia

An explicit feature control approach in structural topology optimization

Weisheng Zhang[1], Xu Guo[1] Wenliang Zhong[1]

[1] State Key Laboratory of Structural Analysis for Industrial Equipment,
Department of Engineering Mechanics,
Dalian University of Technology, Dalian, 116023, P.R. China

1. Abstract
The present paper aims to address a long-standing and challenging problem in structural topology optimization: explicit feature control of the optimal topology. The basic idea is to introduce feature control constraints which are closely related to structural skeleton, which is a key concept in mathematical morphology and a powerful tool for describing structural topologies. Benefit from the ability of structural skeleton in geometrical and topological properties of the shape, the feature control constraints can be represented as local and explicit scheme without any post-processing. To illustrate the effectiveness of the proposed approach, the feature control problem is solved under level set and SIMP framework, respectively. Numerical examples show that the proposed approach does have the capability to give a complete control of the feature size of an optimal structure in an explicit and local way.
2. Keywords: Topology optimization; Feature control; Level-set; SIMP; Structural skeleton.

3. Introduction

Topology optimization of continuum structures, which is, in its mathematically nature, a discrete optimal control problem of the coefficients of partial differential equations in infinite dimensional space, is the most challenging structural optimization problem [1].
One long standing problem in structural topology optimization, which is closely related to regularization, is feature control of optimal structural topology [2-6]. More recently, Guo and Zhang et al.[7,8] proposed two explicit and local approaches for feature control in optimal topology designs.
In the present paper, we intend to discuss how to carry out local and explicit feature control in structural topology optimization under level-set and SIMP-based computational framework, respectively.

4. Mathematical foundation

In order to give a precise feature control of a structure, it is necessary to define the minimum/maximum length scale in a mathematical rigorous way. In the following, this will be achieved by introducing the concept of structural skeleton of a given structure.
Definition 1. The minimum/maximum length scale of a structure under level set framework
In the present paper, the minimum length scale of a domain Ω is defined as

$$d^{\min-\mathrm{ls}}(\Omega)=\min_{\boldsymbol{x}\in\mathcal{MS}(\Omega)}\ \min_{\substack{\boldsymbol{y},\boldsymbol{z}\in\mathcal{CP}(\boldsymbol{x})\\ \boldsymbol{yz}\cap\mathcal{MS}(\Omega)\neq\emptyset}}\|\boldsymbol{y}-\boldsymbol{z}\|, \tag{1}$$

where $\mathcal{CP}(\boldsymbol{x})=\{\boldsymbol{y}|\boldsymbol{y}\in\operatorname{Arg\,min}_{\boldsymbol{z}\in\partial\Omega}\|\boldsymbol{z}-\boldsymbol{x}\|\}$ is the set of closest points of $\boldsymbol{x}\in\mathcal{MS}(\Omega)$ on $\partial\Omega$ and $\boldsymbol{yz}$ denotes the line segment with two end points $\boldsymbol{y}$ and $\boldsymbol{z}$, respectively. $\mathcal{MS}(\Omega)$ is the medial surface of a closed and bounded domain Ω. Accordingly, the maximum length scale of a domain Ω is defined as

$$d^{\max-\mathrm{ls}}(\Omega)=\max_{\boldsymbol{x}\in\mathcal{MS}(\Omega)}\max_{\boldsymbol{y},\boldsymbol{z}\in\mathcal{CP}(\boldsymbol{x})}\|\boldsymbol{y}-\boldsymbol{z}\|, \tag{2}$$

Under level set framework and based on the above definitions, we have the following propositions which constitute the mathematical foundation of the proposed approach.
Proposition 1. If $\min_{\boldsymbol{x}\in\mathcal{MS}(\Omega)}\phi^{\mathrm{SDF}}(\boldsymbol{x})\geq\underline{d}$, then $d^{\min-\mathrm{ls}}(\Omega)\geq 2\underline{d}$.
Proposition 2. If $\max_{\boldsymbol{x}\in\mathcal{MS}(\Omega)}\phi^{\mathrm{SDF}}(\boldsymbol{x})\leq\bar{d}$, then $d^{\max-\mathrm{ls}}(\Omega)\leq 2\bar{d}$.
Here, $\phi^{\mathrm{SDF}}(\boldsymbol{x})$ is the so-called signed distance level set function.
Based on the above definitions and propositions, it becomes clear that the minimum and maximum length scale of a domain Ω can be completely controlled by imposing lower and upper bounds on the values of its signed distance function associated with the points in $\mathcal{MS}(\Omega)$.
Definition 2. The minimum/maximum length scale of a structure under SIMP framework
In order to differentiate between level set and SIMP description, the structural skeleton is defined as $\mathcal{SS}(\Omega)$ under

SIMP framework. Then the minimum length scale $d^{\min}(\Omega)$ and maximum length scale $d^{\max}(\Omega)$ of Ω can be defined as

$$d^{\min-\mathrm{s}}(\Omega) = \inf_{\boldsymbol{x}\in\mathcal{SS}(\Omega)} D(\boldsymbol{x}) \tag{3}$$

and

$$d^{\max-\mathrm{s}}(\Omega) = \sup_{\boldsymbol{x}\in\mathcal{SS}(\Omega)} D(\boldsymbol{x}), \tag{4}$$

respectively, where $D(\boldsymbol{x})$ is defined as

$$D(\boldsymbol{x}) = \sup_{r\geq 0}\{2r|\mathcal{B}(\boldsymbol{x},r)\subseteq\Omega\}, \quad \text{for } \forall\boldsymbol{x}\in\mathcal{SS}(\Omega). \tag{5}$$

In Eq.(3), $\mathcal{B}(\boldsymbol{x},r)$ denotes a closed ball centered at $\boldsymbol{x}$ with radius r.
If the topology of a structure can be represented by a binary bitmap, numerous well established image processing techniques can be employed to extract its skeleton.

5. Problem formulation with feature control

Armed with above facts, the following problem formulation is proposed for topology optimization of continuum structures with feature control under level set-based framework:

$$\begin{aligned}
&\text{Find } \phi^{\mathrm{SDF}}(\boldsymbol{x}),\ \boldsymbol{u}(\boldsymbol{x})\\
&\text{Min } \quad I = I(\phi^{\mathrm{SDF}},\boldsymbol{u})\\
&\text{s.t.}\\
&\int_{\mathrm{D}} H(\phi^{\mathrm{SDF}})\mathbb{E}:\boldsymbol{\varepsilon}(\boldsymbol{u}):\boldsymbol{\varepsilon}(\boldsymbol{v})\mathrm{dV} = \int_{\mathrm{D}} H(\phi^{\mathrm{SDF}})\boldsymbol{f}\cdot\boldsymbol{v}\mathrm{dV} + \int_{\Gamma_{\mathrm{t}}}\boldsymbol{t}\cdot\boldsymbol{v}\mathrm{dS}, \qquad \forall\boldsymbol{v}\in\mathcal{U}_{\mathrm{ad}},\\
&\int_{\mathrm{D}} H(\phi^{\mathrm{SDF}})\,\mathrm{dV}\leq\bar{V},\\
&\phi^{\mathrm{SDF}}(\boldsymbol{x})\geq\underline{d}, \quad \forall\boldsymbol{x}\in\mathcal{MS}(\Omega),\\
&\phi^{\mathrm{SDF}}(\boldsymbol{x})\leq\bar{d}, \quad \forall\boldsymbol{x}\in\mathcal{MS}(\Omega),\\
&\boldsymbol{u}=\bar{\boldsymbol{u}}, \quad \text{on } \Gamma_{\mathrm{u}}.
\end{aligned} \tag{6}$$

In Eq. (6), D is a prescribed design domain in which optimal material distribution is sought for. $\boldsymbol{f}$ and $\boldsymbol{t}$ denote the body force density in D and the traction force on Neumann boundary Γ_{t}, respectively. $\bar{\boldsymbol{u}}$ is the prescribed displacement on Dirichlet boundary Γ_{u}. The symbol $\boldsymbol{\varepsilon}$ denotes the second order linear strain tensor. $\mathbb{E}^k = \mathrm{E}^s/(1+(\nu)^s)[\mathbb{I}+\nu^s/(1-2\nu^s)\delta\otimes\delta]$ ($\mathbb{I}$ and δ denote the fourth and second order identity tensor, respectively) is the fourth order isotropic elasticity tensor of the solid material with E^{s} and ν^s denoting the corresponding Young's modulus and Poisson's ratio, respectively. $\boldsymbol{u}$ and $\boldsymbol{v}$ are the displacement field and the corresponding test function defined on D with $\mathcal{U}_{\mathrm{ad}} = \{\boldsymbol{v}|\ \boldsymbol{v}\in\mathbf{H}^1(\mathrm{D}), \boldsymbol{v}=\mathbf{0} \text{ on } \Gamma_{\mathrm{u}}\}$. The function H is such that $H(x)=1, \text{if } x\geq 0;\ H(x)=1.0e-06, \text{otherwise}.$ I and $\bar{V}$ are the objective functional and prescribed upper bound of the solid material. They are all functional of ϕ^{SDF} and $\boldsymbol{u}$. As discussed in the previous section, the constraints imposed on the signed distance ϕ^{SDF} play the role of feature control. With use of these constraints, the minimum and maximum length scales of the obtained structure will be greater than $2\underline{d}$ and less than $2\bar{d}$, respectively.
In the SIMP framework, the optimization problem can be formulated as follows:

$$\begin{aligned}
&\text{Find } \boldsymbol{\rho}=(\rho_1,\rho_2,\cdots,\rho_n)^{\top},\boldsymbol{u}\\
&\text{Min } \quad C=\boldsymbol{u}^{\top}\boldsymbol{K}(\boldsymbol{\rho})\boldsymbol{u}\\
&\text{s.t.}\\
&\boldsymbol{K}(\boldsymbol{\rho})\boldsymbol{u}=\boldsymbol{f},\\
&V(\boldsymbol{\rho})=\sum_{i=1}^{n}\rho_i v_i\leq\bar{V},\\
&g_1(\boldsymbol{\rho})=\sum_{j\in I_{\min}}(\rho_j-1)^2\leq\epsilon_1,\\
&g_2(\boldsymbol{\rho})=\sum_{k\in I_{\max}}(\rho_k-\rho_{\min})^2\leq\epsilon_2,\\
&\rho_{\min}\leq\rho_i\leq 1, \qquad \forall\, i=1,\dots,n.
\end{aligned} \tag{7}$$

In Eq. (7), $\boldsymbol{\rho}$ is the vector of the design variables with ρ_i and v_i denoting the density and volume of the i-th element. The symbol n denotes the total number of finite element used for discretizing the prescribed design domain D. $\boldsymbol{K}=\sum_{i=1}^{n}\rho_i^p\boldsymbol{K}_{\mathbf{0}}$ (p is the penalization index and $p=3$ is adopted in the present study) is the global stiffness matrix with $\boldsymbol{K}_0$ representing the element stiffness matrix corresponding to $\rho_i = 1$. $\rho_{\min}$ is the lower bound of the element density. $g_1 \leq \epsilon_1$ and $g_2 \leq \epsilon_2$ are the minimum and maximum length scale constraint, respectively. $\boldsymbol{f}$ and $\boldsymbol{u}$ are the external load and the displacement field, respectively. In Eq. (3.1), $I_{\min}$ and $I_{\max}$ are two index sets such that

$$I_{\min} = \left\{ j \middle| j \in \{1, \dots, n\}, \Omega_j \in \bigcup_{x \in \mathcal{SS}(\Omega)} \mathcal{B}(\boldsymbol{x}, \underline{d}) \right\} \tag{8}$$

and

$$I_{\max} = \left\{ k \middle| k \in \{1, \dots, n\}, \Omega_k \notin \bigcup_{x \in \mathcal{SS}(\Omega)} \mathcal{B}(\boldsymbol{x}, \bar{d}) \right\}, \tag{9}$$

respectively.

6. Numerical solution aspects

In this section, numerical solution aspects of the proposed method will be discussed in detail.

4.1. The Identification of $\mathcal{MS}(\Omega)$ and $\mathcal{SS}(\Omega)$

From the above discussions, it is obvious that the key point for solving the optimization problem in Eq. (6) and (7) is to identify the medial surface of Ω, i.e, $\mathcal{MS}(\Omega)$ and $\mathcal{SS}(\Omega)$. In the present work, as suggested in [9], the following approximated Laplacian and then a line sweeping algorithm are applied to ϕ^{SDF} sequentially to identify the points in $\mathcal{MS}(\Omega)$ approximately as

$$\mathcal{MS}(\Omega) \cong \{\boldsymbol{x} | \phi^{\mathrm{SDF}}(\boldsymbol{x}) > 0, |\nabla^2 \phi^{\mathrm{SDF}}(\boldsymbol{x})| > 0\}, \tag{10}$$

with

$$\nabla^2 \phi_{ij}^{\mathrm{SDF}} \cong \phi_{i+1,j}^{\mathrm{SDF}} + \phi_{i-1,j}^{\mathrm{SDF}} + \phi_{i,j+1}^{\mathrm{SDF}} + \phi_{i,j-1}^{\mathrm{SDF}} - 4\phi_{i,j}^{\mathrm{SDF}}. \tag{11}$$

Taking the possible numerical error into consideration, $\mathcal{MS}^{\epsilon}(\Omega)$ defined as

$$\mathcal{MS}^{\epsilon}(\Omega) \cong \left\{ \boldsymbol{x} \middle| \phi^{\mathrm{SDF}}(\boldsymbol{x}) > 0, \left| \nabla^2 \phi^{\mathrm{SDF}}(\boldsymbol{x}) / \max_{\boldsymbol{x} \in \Omega} |\nabla^2 \phi^{\mathrm{SDF}}(\boldsymbol{x})| \right| > \epsilon \right\}, \tag{12}$$

where ϵ is a small positive number, is used in numerical implementation to guarantee the robustness of the solution process. In fact, $\mathcal{MS}^{\epsilon}(\Omega)$ constitutes a narrow band around $\mathcal{MS}(\Omega)$.

In SIMP framework, we propose to introduce the following projection operator to transform the gray-valued density field (i.e., $\rho(\boldsymbol{x})$) into a pure black-and-white density field (i.e., $\hat{\rho}(\boldsymbol{x})$) used for extracting the structural skeleton:

$$\hat{\rho}(\boldsymbol{x}) = \begin{cases} 1, & if\ \rho(\boldsymbol{x}) \geq \bar{\rho}, \\ 0, & \text{otherwise}, \end{cases} \tag{13}$$

where $\bar{\rho}$ is a threshold value for density projection. In the present work, we will make use of Otsu method [10] to determine $\bar{\rho}$ in every optimization step adaptively in order to avoid misrecognition. Once the binary density field is identified, the iterative skeleton algorithm [11] can be adopted to identify the structural skeleton.

4.1. The sensitivity analysis

In Eq.(6), the existence of a large number of point-wise feature control constraints makes the direct solution approaches computationally intractable. In the present paper, the technique proposed in [12] is employed to transfer the local feature control constraints into a global one in a mathematically equivalent way. This can be achieved as follows. By defining

$$g^{\epsilon} = \int_{\mathcal{MS}^{\epsilon}(\Omega)} \mathcal{H}\left(\phi^{\mathrm{SDF}}(\boldsymbol{x}), \underline{d}, \bar{d}\right) \mathrm{dV}, \tag{14}$$

with

$$\mathcal{H}\left(\phi^{\mathrm{SDF}}(\boldsymbol{x}), \underline{d}, \bar{d}\right) = \begin{cases} \left(\phi^{\mathrm{SDF}} - \bar{d}\right)^2, & \text{if } \phi^{\mathrm{SDF}} > \bar{d}, \\ \left(\phi^{\mathrm{SDF}} - \underline{d}\right)^2, & \text{if } \phi^{\mathrm{SDF}} < \underline{d}, \\ 0, & \text{otherwise}. \end{cases} \tag{15}$$

The basic assumptions behind shape sensitivity analysis are such that both $\mathbb{E}$ and $\boldsymbol{t}$ are spatial invariant, i.e., $(\mathbb{E})' = \mathbb{O}$ and $(\boldsymbol{t})' = \boldsymbol{0}$. It is also assumed that $\bar{\boldsymbol{u}} = \boldsymbol{0}$ on Γ_{u} as well as the part of the Neumann boundary Γ_{t} where $\boldsymbol{t} \neq 0$ are non-designable. For g^{ϵ}, we have

$$(\dot{g^{\epsilon}}) = \int_{\mathcal{MS}^{\epsilon}(\Omega)} \frac{\partial \mathcal{H}\big(\phi^{\mathrm{SDF}}(\boldsymbol{x}), \underline{d}, \bar{d}\big)}{\partial t} \mathrm{dS} + \int_{\mathcal{MS}^{\epsilon}(\Omega)} (-v_n^{\mathcal{MS}}) \boldsymbol{n}^{\mathcal{MS}} \cdot \nabla \mathcal{H}\big(\phi^{\mathrm{SDF}}(\boldsymbol{x}), \underline{d}, \bar{d}\big) \mathrm{dS} + \int_{\mathcal{MS}^{\epsilon}(\Omega)} (-v_n^{\mathcal{MS}}) \kappa^{\mathcal{MS}} \mathcal{H}\big(\phi^{\mathrm{SDF}}(\boldsymbol{x}), \underline{d}, \bar{d}\big) \mathrm{dS}, \tag{16}$$

where $\boldsymbol{n}^{\mathcal{MS}}$ and $\kappa^{\mathcal{MS}}$ are the outward normal vector and curvature of $\mathcal{MS}(\Omega)$, respectively. In Eq. (18), $v_n^{\mathcal{MS}}$ is the outward normal velocity of $\mathcal{MS}(\Omega)$.

Since

$$\frac{\partial \mathcal{H}\big(\phi^{\mathrm{SDF}}(\boldsymbol{x}), \underline{d}, \bar{d}\big)}{\partial t} = \mathcal{H}'\big(\phi^{\mathrm{SDF}}(\boldsymbol{x}), \underline{d}, \bar{d}\big) \frac{\partial \phi^{\mathrm{SDF}}(\boldsymbol{x})}{\partial t}, \tag{17}$$

$$\nabla \mathcal{H}\big(\phi^{\mathrm{SDF}}(\boldsymbol{x}), \underline{d}, \bar{d}\big) = \mathcal{H}\big(\phi^{\mathrm{SDF}}(\boldsymbol{x}), \underline{d}, \bar{d}\big) \nabla \phi^{\mathrm{SDF}}(\boldsymbol{x}), \tag{18}$$

where

$$\mathcal{H}'\big(\phi^{\mathrm{SDF}}(\boldsymbol{x}), \underline{d}, \bar{d}\big) = \begin{cases} 2\big(\phi^{\mathrm{SDF}} - \bar{d}\big), & \text{if } \phi^{\mathrm{SDF}} > \bar{d}, \\ 2\big(\phi^{\mathrm{SDF}} - \underline{d}\big), & \text{if } \phi^{\mathrm{SDF}} < \underline{d}, \\ 0, & \text{otherwise.} \end{cases} \tag{19}$$

Since $\partial \phi^{\mathrm{SDF}} / \partial t = -v_n^{\phi^{\mathrm{SDF}}} |\nabla \phi^{SDF}|$ and $|\nabla \phi^{\mathrm{SDF}}| = 1$, we finally arrive at the result that

$$(\dot{g^{\epsilon}}) = \int_{\mathcal{MS}^{\epsilon}(\Omega)} \frac{\partial \mathcal{H}\big(\phi^{\mathrm{SDF}}(\boldsymbol{x}), \underline{d}, \bar{d}\big)}{\partial t} \mathrm{dV} + \int_{\partial \mathcal{MS}^{\epsilon}(\Omega)} (-v_n^{\mathcal{MS}^{\epsilon}}) \mathcal{H}\big(\phi^{\mathrm{SDF}}(\boldsymbol{x}), \underline{d}, \bar{d}\big) \mathrm{dS} = \int_{\mathcal{MS}^{\epsilon}(\Omega)} \mathcal{H}'\big(\phi^{\mathrm{SDF}}(\boldsymbol{x}), \underline{d}, \bar{d}\big) \left(-v_n^{\phi^{\mathrm{SDF}}}\right) \mathrm{dV} + \int_{\partial \mathcal{MS}^{\epsilon}(\Omega)} (-v_n^{\mathcal{MS}^{\epsilon}}) \mathcal{H}\big(\phi^{\mathrm{SDF}}(\boldsymbol{x}), \underline{d}, \bar{d}\big) \mathrm{dS} \tag{20}$$

At this position, it is worthy of noting that $v_n^{\mathcal{MS}^{\epsilon}}$ is not an independent quantity that can be chosen freely. In fact, it is dependent on $v_n^{\phi^{\mathrm{SDF}}}$ in an implicit way. Therefore, it is somewhat difficult to determine the descent ensuring velocity field of g_1 or g_1^{ϵ} in the same way as in traditional level set methods. In our numerical implementation, g^{ϵ} is employed to control the minimum structural feature length scale. Under this circumstance, by neglecting the second term in Eq.(20). Numerical experiments showed that the above treatment is effective to deal with the feature control constraints.

The velocity fields associated with g^{ϵ} is only defined on $\mathcal{MS}^{\epsilon}(\Omega)$, which is only a subset of D (i.e., $\mathcal{MS}^{\epsilon}(\Omega) \subset \Omega \subset \mathrm{D}$). The evolution of ϕ^{SDF}, however, requires the velocity field on all points in D. In the present study, the PDE-based velocity extension method proposed is employed to extend the velocity fields associated with g^{ϵ} defined primarily on $\mathcal{MS}^{\epsilon}(\Omega)$ to D.

Under SIMP framework, by assuming that the index sets I_{min} and I_{max}, do not change before and after the perturbations of design variables, it holds that $\partial g_1 / \partial \rho_j = 2\big(\rho_j - 1\big), \forall\, j \in I_{\mathrm{min}}$, $\partial g_1 / \partial \rho_j = 0, \forall\, j \notin I_{\mathrm{min}}$ and $\partial g_2 / \partial \rho_k = 2(\rho_k - \rho_{\mathrm{min}})$, $\forall\, k \in I_{\mathrm{max}}, \partial g_2 / \partial \rho_k = 0$, $\forall\, k \notin I_{\mathrm{max}}$, respectively.

7. Numerical examples

In this section, the proposed approach is applied to several benchmark examples of topology optimization to illustrate its effectiveness for feature control. In the following tested examples, the Young's modulus and Poisson's ratio of the solid material are taken as $\mathrm{E^s} = 1$ and $\mathrm{\nu^s} = 0.3$, respectively unless otherwise stated. Under SIMP framework, the lower bound of the density variable is $\rho_{\mathrm{min}} = 10^{-2}$ in numerical implementation. Unless otherwise stated, the relaxation parameters ϵ_1 and ϵ_2 are set to be 10^2 initially and reduced to 1 within 20 iterative steps.

First，we test the feature control capability of Eq.(6) under level set framework. As shown in Fig. 1, the design domain is 2×1 rectangular sheet with its left side clamped. A unit vertical load is applied at the middle point of the right side of the sheet. The design domain is discretized by an 120×60 FEM mesh.

The structure is optimized to minimize the mean compliance of the structure under the available solid material constraint $\mathrm{V_s} \leq 0.5|\mathrm{D}|$. The parameters for the feature controlled optimization are $\underline{d} = 0.5 \times \min(\Delta x, \Delta y)$, $\bar{d} = 1.5 \times \min(\Delta x, \Delta y)$ and $\epsilon = 0.6$, respectively. Fig. 2 shows the optimal topologies without and with feature control constraints. The obtained numerical results indicate that the proposed approach does have the capability of complete feature size control and the optimal solution obtained with feature size constraints may be quite different from that obtained without considering feature size constraints. The value of the objective functional of the feature controlled optimal design is $I = 85.12$ with solid volume $\mathrm{V_s} = 0.5|\mathrm{D}|$ while the corresponding values of the no controlled design are $I = 62.41$ and $V_s = 0.5|D|$, respectively.

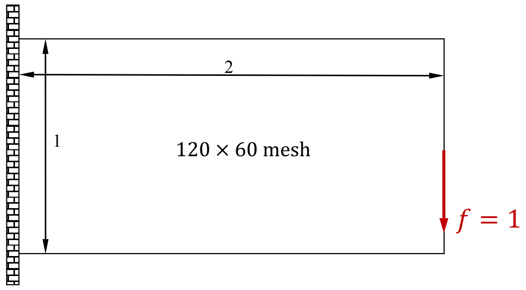

Fig. 1 The design domain of the short beam example

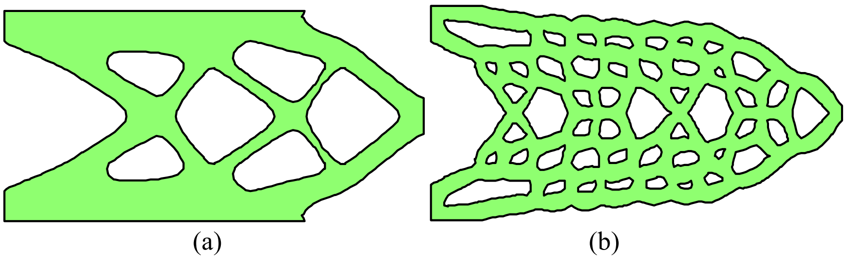

Fig.2. The optimal design of the short beam example：
(a) without feature control (b) with feature control

Under SIMP framework, the heat conduction problem shown in Fig. 3, where the objective is to maximize the heat transfer capacity, is examined under minimum length scale control constraint. The design domain where distributed unit thermal loading uniformly applied is discretized with a 100×100 FEM mesh and the temperature of left-middle side is set to 0, as shown in Fig. 3. When the upper bound of the available solid material volume is $\bar{V} = 0.5$, the optimized structure without length scale constraints is shown in Fig. 4a. It can be seen that this optimal design is unfavorable for manufacturing due to the existence of a large number of fins with small thickness. Next, the same problem is reconsidered with length scale constraint being taken into consideration. It is required that the minimum length scale of the thermal fins should be greater than $\underline{d} = 7 \times \min(\Delta x, \Delta y)$. The optimized design and the corresponding structural skeleton are shown in Fig. 4b. From Fig. 4b, it can be seen that compared with the design shown in Fig. 4a, several main heat transfer paths are still retained in the optimal design subjected to length scale constraint. However, the fins with small widths have been eliminated. The optimal design shown in Fig. 4b is more reasonable from manufacturability point of view. Accordingly, the value of the objective function has been decreased from 186.63 to 133.35, due to the existence of length scale constraint.

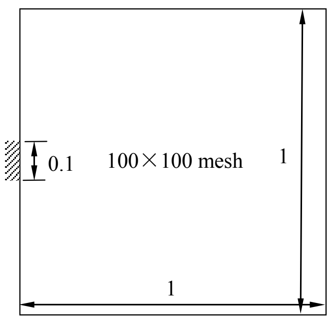

Fig. 3 The design domain of the heat conduction example.

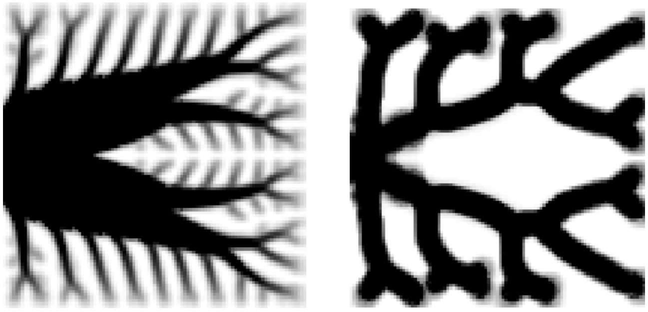

(a) (b)

Fig. 4 The optimized design of the heat conduction problem:
(a)without feature control (b) with with control

8. Concluding remarks

In the present paper, two problem formulations and the corresponding numerical solution algorithm for feature control in optimal topology designs are proposed under level set framework and SIMP framework, respectively. Our methods are established based on the concept of structural skeleton, which has been well addressed in the field of image processing. Compared with the existing feature control approaches, the advantages of the proposed methods are such that they are local and explicit feature control schemes without resorting to any post-processing or continuation treatment. Numerical examples show that the proposed methods can give a complete (i.e., minimum and maximum length scales) control of the feature sizes in the optimized structures.

9. Acknowledgements

The financial supports from the National Natural Science Foundation (10925209, 91216201, 11372004, 11402048), 973 Project of China (2010CB832703), Program for Changjiang Scholars, Innovative Research Team in University (PCSIRT) and 111 Project (B14013) are also gratefully acknowledged.

10. References

[1] M.P. Bendsoe and O. Sigmund, *Topology Optimization: Theory, Methods and Applications*, Springer-Verlag, Berlin, 2003.
[2] J. Petersson, O. Sigmund, Slope constrained topology optimization, *International Journal for Numerical Methods in Engineering,* 41, 1417–1434, 1998.
[3] T.A. Poulsen, A new scheme for imposing minimum length scale in topology optimization, *International Journal for Numerical Methods in Engineering,* 57,741–760, 2003.
[4] J.K. Guest, Achieving minimum length scale in topology optimization using nodal design variables and projection functions, *International Journal for Numerical Methods in Engineering,* 61, 238-254, 2004.
[5] J.K. Guest, Imposing maximum length scale in topology optimization, *Structural and Multidisciplinary Optimization,* 37, 463-473, 2009.
[6] S.K. Chen, M.Y. Wang, A.Q. Liu, Shape feature control in structural topology optimization, *Computer Aided Design*, 40, 951-962, 2008.
[7] W.S. Zhang, X. Guo, W.L. Zhong. An explicit length scale control approach in SIMP-based topology optimization, *Computer Methods in Applied Mechanics and Engineering*, 282, 71-86, 2014.
[8] X. Guo, W.S. Zhang, W.L. Zhong. Explicit feature control in structural topology optimization via level set method, *Computer Methods in Applied Mechanics and Engineering*, 272, 354-378,2014.
[9] A.A. Eftekharian, H.T. Llies, Distance functions and skeletal representations of rigid and non-rigid planar shapes, *Computer Aided Design*, 41, 856-876,2009.
[10] N. Otsu, A threshold selection method from gray-level histograms, *IEEE Transactions on Systems, Man, and Cybernetics*, 9, 62-66,1979.
[11] A. Rosenfeld, L.S. Davis, A note on thinning, *IEEE Transactions on Systems, Man, and Cybernetics*, 25,226-228,1976.
[12] W.S. Zhang, X. Guo, M.Y. Wang, P. Wei, Optimal topology design of continuum structures with stress concentration alleviation via level set method, *International Journal for Numerical Methods in Engineering*. 93, 942–959, 2013.